Ion-molecule reactions in quadrupole ion trap mass spectrometry: implications for lightweight gas analysis

Andrew K. Ottens[a,*], C. Richard Arkin[b],
Timothy P. Griffin[c], Peter T. Palmer[d], W.W. Harrison[a]

[a] *Department of Chemistry, University of Florida, PO Box 117200, Gainesville, FL 32611-7200, USA*
[b] *ASRC Aerospace, Mailstop ASRC-14, Kennedy Space Center, FL 32899, USA*
[c] *National Aeronautics and Space Administration, Mailstop YA-F2-C, Kennedy Space Center, FL 32899, USA*
[d] *San Francisco State University, Department of Chemistry and Biochemistry, San Francisco, CA 94132, USA*

Abstract

The novel application of a quadrupole ion trap mass spectrometer (QITMS) to permanent gas analysis was recently presented by our laboratory. The quantitative performance of the QITMS equaled or surpassed that of other mass analyzers evaluated; however, concern was raised as to the impact of ion-molecule reactions observed within the ion trap. Hydrogen, helium, oxygen, and argon, four permanent gases currently monitored during Space Shuttle launch preparations by the National Aeronautics and Space Administration, were examined in their reactions with common atmospheric and mass spectrometer background components. Rapid charge-exchange and protonation reactions occurred. Greater than 99.8% of hydrogen and 98% of helium ions trapped are lost during a scan cycle predominately through reactions with background nitrogen. The neutralization rate of argon ions varied with water concentration, while increased concentrations of all three gases inflated the oxygen ion signal intensity through charge-exchange. Although such dramatic effects challenge the analytical sensitivity and robustness of QITMS for permanent gas analysis, through proper understanding and control of relevant experimental conditions the QITMS can still function in monitoring applications.
© 2004 Elsevier B.V. All rights reserved.

Keywords: Ion trap; Ion-molecule reaction; Charge-exchange; Proton transfer; Permanent gas analysis

1. Introduction

The National Aeronautics and Space Administration (NASA) has used mass spectrometers to detect cryogenic fuel leaks since the start of the Space Shuttle program in 1981 [1]. Mass spectrometers offer low detection limits, stable readings, with fast analyses, and were effective in detecting cryogenic fuel leaks on numerous occasions throughout the years (STS6 in 1985, STS35 and STS38 in 1989, and STS93 in 2000) [1,2]. However, due to fragility and bulkiness, NASA has historically been limited to using only two remotely located systems [3], which precludes real-time simultaneous monitoring of all Space Shuttle compartments and excludes leak detection during the last critical minute prior to launch. Recognizing these limitations, NASA sought a new compact, rugged, and less costly mass spectrometer so that multiple systems could be situated up-close to the Space Shuttle providing rapid monitoring of all internal compartments throughout pre-launch until lift-off. The advanced hazardous gas detection (AHGD) project was initiated to meet this directive. As part of this work, a compact quadrupole ion trap mass spectrometer (QITMS) was designed, fulfilling NASAs performance requirements for monitoring hydrogen, helium, oxygen, and argon in a nitrogen purged atmosphere [4,5].

* Corresponding author. Present address: Department of Neuroscience, University of Florida, PO Box 100244, Gainesville, FL 32610-0244, USA. Tel.: +1 352 392 8060; fax: +1 352 392 8347.

E-mail addresses: aottens@mbi.ufl.edu (A.K. Ottens), richard.arkin-1@ksc.nasa.gov (C.R. Arkin), timothy.p.griffin@nasa.gov (T.P. Griffin), palmer@sfsu.edu (P.T. Palmer), harrison@chem.ufl.edu (W.W. Harrison).
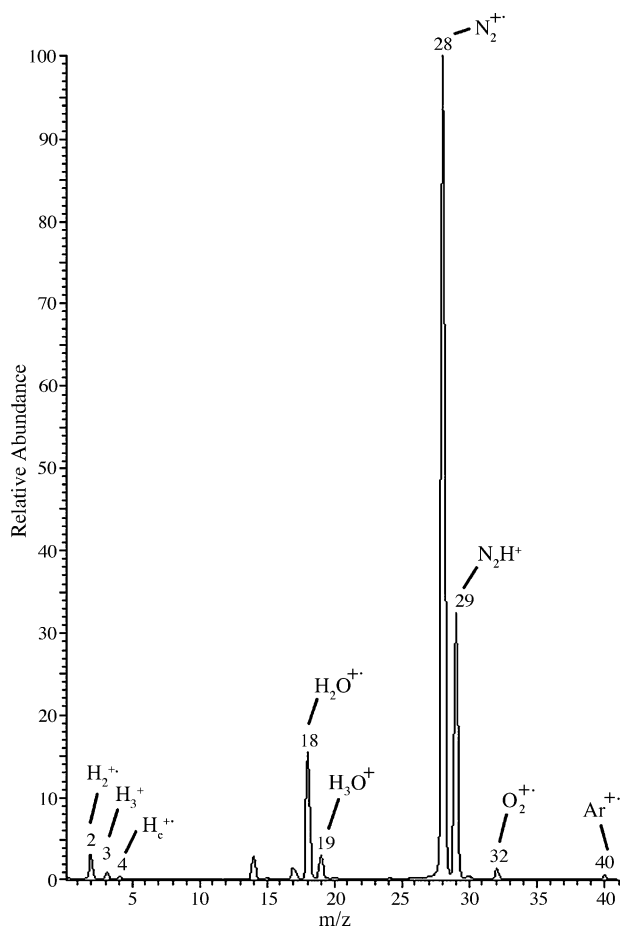
Fig. 1. Mass spectrum of lightweight gases analyzed by the QITMS gas analyzer developed at the University of Florida. Ion signals at m/z 3 (H_3^+), 19 (H_3O^+), and 29 (N_2H^+) show that ion-molecule reactions are occurring within the ion trap, affecting QITMS quantitative performance.

Table 1
Energy values associated with ion-molecule reactions for ions and neutrals of interest

Ions/neutrals of interest		RE[a] (eV)	IE[b] (eV)	PA[c] (eV)
$H_2^{\bullet+}$	H_2	16.4–17.4	15.4	4.377
H_3^+		9.2		
$He^{\bullet+}$	He	24.6	24.6	1.843
$H_2O^{\bullet+}$	H_2O	12.4	12.6	7.16
H_3O^+		6.4		
$N_2^{\bullet+}$	N_2	15.3	15.6	5.118
N_2H^+		8.5		
$O_2^{\bullet+}$	O_2	11.2–11.3	12.1	4.36
$Ar^{\bullet+}$	Ar	15.8	15.8	3.827

[a] Recombination energy (RE) [6,15,16].
[b] Ionization energy (IE) of neutral [17].
[c] Proton affinity (PA) of neutral [18].

The concept of the quadrupole ion store or QUISTOR, first proposed by Lawson and Todd [10,11], was used explicitly for reaction studies, leading to the development of the low pressure CI source, where time (not pressure) was used to provide a sufficient number of collisions. Unwanted reactions in this process would affect quantitative performance by changing analyte ion signals and adding chemical noise such that even before its commercialization, QITMS was known to be affected by gas phase reactions.

1.1. Ion-molecule reactions

The average velocity of an ion inside the ion trap with $q_z = 0.25$ is 7 m/ms (see equation in [12]), and at an ambient ion trap pressure of 7×10^{-6} Torr the mean free path is 7 m. These parameters result in a collision every ms, allowing for numerous reactions within a 10–20 ms analysis time. There are three possible ion-molecule reaction pathways: charge-exchange, proton transfer, and hydrogen-atom transfer. Charge-exchange involves transfer of an electron from the ambient neutral to the analyte ion radical [6,13–16]. The reaction is exothermic when the recombination energy (RE) of the ion radical is greater than the ionization energy (IE) of the neutral (RE and IE values of interest are listed in Table 1). Brønsted acid ions, such as H_3^+, are formed by proton transfer when the conjugate neutral base has a higher proton affinity (PA) [6,18] (see Table 1 for PA converted to eV from Table 1 of [18]). Self-protonation also occurs since the PA value of a neutral gas phase acid is greater than that of its conjugate ion. The third less understood reaction involves the transfer of a hydrogen atom from a molecule to an ion radical [6,19–24], the energetics of which are similar to proton transfer, but the exact mechanism is still in dispute.

1.2. Kinetics of ion-molecule reactions

Ions will react within a QITMS given exothermic conditions and time. Studying reactions between analytes and resident neutrals is required to determine QITMS effec-

QITMS mass spectra, as in the case of Fig. 1, showed unexpected ion signals at m/z 3, 19, and 29 which were not readily observed on other non-trapping mass analyzers evaluated for the AHGD project. These peaks represented $(M+H)^+$ ions of hydrogen, water, and nitrogen, respectively. The proton transfer reactions leading to these ions have been characterized by mass spectrometry since 1916 when the H_3^+ ion at m/z 3 was first isolated [6]. In the 1950s, improved mass spectrometry technology and the advent of chemical ionization (CI) prompted further study of ion-molecule reactions. Three instrument configurations were commonly used: (1) tandem-in-space mass spectrometry (e.g., sector and triple quadrupole); (2) drift tube methods with either spectroscopic or mass spectrometric detection; and (3) tandem-in-time mass spectrometers (e.g., Fourier-transform ion cyclotron resonance and QITMS) [7]. Using tandem-in-space mass spectrometry, reactions were controlled by adjusting the gas pressure in the collision cell, while drift tube methods (e.g., selected ion flow tube, SIFT) monitored reaction in time. Tandem-in-time instruments were advantageous in that reactions could be controlled with respect to time and pressure [8,9].

tiveness for gas monitoring applications. Kinetics of ion-molecule reactions can be explored conveniently inside the ion trap by adjusting ion storage time [12,25]. Rate constants (k) can be determined assuming pseudo-first-order reactions where $[A^+] \ll [B]$. The rate constant can be expressed as the rate equation

$$k = -\ln \frac{[A^+]_t}{[A^+]_0} \frac{1}{t[B]} \tag{1}$$

where the ratio between the initial concentration, $[A^+]_0$, and final concentration, $[A^+]_t$, is replaced by a ratio of initial and final ion signal intensities. The significance of a reaction on QITMS performance increases with reaction rate, which can be approximated by the magnitude of the rate constant, where values on the order of 10^{-9} cm^3/s molecule are typical for fast reactions [24,26].

Rate constants can be approximated using ion-induced dipole collisional rate theory by Eq. (2) [6,27]:

$$k_L = v\sigma_c(v) = 2\pi q \left(\frac{\alpha}{\mu} \right)^{1/2} \tag{2}$$

The Langevin rate constant, k_L, is related to the relative velocity (v), and collisional cross-section (σ_c), or the ions charge (q), the neutrals polarizability (α), and the reduced mass (μ) of the ion–neutral pair. This approximation is accurate for non-polar neutrals (most permanent gases), but not for water which has a significant dipole (μ_D) increasing the collisional cross-section. Dipole moments are accounted for in average dipole orientation (ADO) theory, where the rate constant is approximated as

$$k_{ADO}(T) = \left(\frac{2\pi q}{\sqrt{\mu}} \right) \left[\sqrt{\alpha} + C\mu_D \left(\frac{2}{\pi k T} \right)^{1/2} \right] \tag{3}$$

which is dependent on the absolute temperature T in K (k is the Boltzmann's constant). The value C is a dipole-locking constant that is dependent on the value $\mu_D/\sqrt{\alpha}$, which for water is 0.25 at 300 K (Fig. 3 on p. 12 of [6], with dipole moment and polarizability values from [17] [6,27,28]. The approximate k values of these two theories provide a reference point for evaluating the accuracy of our measured reaction rates.

1.3. Overview

In this study we explore ion-molecule reactions involving hydrogen, helium, oxygen, argon, and the abundant background gases nitrogen and water. The significance of ion-molecule reactions when monitoring permanent gases by QITMS is discussed. In addition, the results provide a framework to optimize quantitative performance by minimizing effects of ion-molecule reactions.

2. Equipment and methods

Pure gas standards were used for hydrogen, helium, and argon. Oxygen ions were studied from the mass spectrometer background. The following sections discuss the gas delivery method, the calculation of neutral gas density, and a description of QITMS operational parameters.

2.1. Gas delivery setup

All gas standards were produced by BOC Gases (Murray Hill, NJ) to a purity of 99.999%. Two-stage stainless steel cylinder regulators (Matheson, Montgomeryville, PA) provided a constant 20 psig output pressure configured with Swagelok (Solon, OH) QC series quick-disconnect fittings to allow rapid switching of gas lines (1/8 in. OD stainless steel).

One gas stream was admitted by the main inlet of the QITMS through a 0.001 in. inlet orifice. A Granville-Phillips (Hudson, NH) 203 leak valve regulated the gas flow passing through the inlet orifice, evacuated to mTorr pressures by a Varian (Lexington, MA) SH-100 scroll pump. Gas sampled through the inlet orifice exhausted between the ring electrode and the exit endcap directly into the ion trap. A low flow of gas into the ion trap was effectively achieved by this method.

A second gas stream was admitted through an auxiliary port to control the background pressure in the vacuum chamber. The flow stream was controlled by a Granville-Phillips 203 leak valve directly from the gas-cylinder regulator into the vacuum chamber. The gas flow through this inlet was less precise, due to the high-pressure differential across the 203 leak valve. Consequently, a low conductance was required, which significantly increased the time for switching gases. To minimize conductance drifts the leak valve was baked at 200 °C to prevent the condensation of water inside the valve.

2.2. Number density determination

An accurate determination of the reactant neutral's number density within the ion trap was required for kinetics experiments. Assuming Boltzmann distribution the number density (N_d) in molecules/cm^3 of a gas is described by

$$N_d = \frac{C}{k} \frac{P}{T} \tag{4}$$

for a partial pressure P (Torr). The constant $C = 1.33 \times 10^{-4}$ converts Torr to Pa and m to cm, k is the Boltzmann's constant and T the manifold temperature reported in K. Gas pressure admitted via the auxiliary inlet was measured via an attached ion gauge (Granville-Phillips). Ionization correction factors were supplied by the ion gauge manufacturer. Additional correction was required to determine the ion trap pressure. This was accomplished by measuring the difference in gas pressure when admitting through the auxiliary port and through the main inlet for various flow rates. Correlation values were

calculated and applied to determine local ion trap pressure for different gases.

2.3. Custom QITMS and scan functions

The compact QITMS was engineered for permanent gas analysis with details published elsewhere [4]. In brief, a Finnigan (San Jose, CA) ITS-40® model vacuum chamber and ion trap ($r_0 = 1.000$ cm, $z_0 = 0.785$ cm) were mated with the electronics of a Finnigan GCQ® QITMS. The quartz ion trap ring spacers were removed to increase gas conductance through the ion trap. A buffer gas was not employed as it interfered with permanent gas analysis and was not essential for lightweight ion trapping. The RF drive frequency was increased to 2.5 MHz shifting the effective ion analysis range to 2–60 Th as necessary for analyte analysis. The 16-bit GCQ RF control DAC provided high resolution control over the small m/z range, which permitted a 3-time increase in the QITMS analytical scan rate to 16,667 amu/s. The increased scan rate proved advantageous in significantly reducing the time needed to eject ions from the ion trap, whereby mini-

mizing ion signal loss during the analytical scan from ion-molecule reactions.

QITMS operation was optimized for analysis of each of the target gases. The scan function for helium ions is shown in Fig. 2a. The RF amplitude was first held at a low RF amplitude, 104 $V_{(0-p)}$, where the working point was $q_z = 0.363$ for helium ions that were effectively trapped during a 1 ms ionization period. The RF amplitude was then increased to provide better trapping conditions for higher m/z product ions (e.g., 14, 18, and 28) produced during the reaction period varied from 0 to 30 ms over 14 scans. The RF amplitude was than ramped to eject ions between 4 and 32 Th within 1.68 ms.

The hydrogen ion scan function is shown in Fig. 2b. As with helium a low RF amplitude (78 $V_{(0-p)}$) was required during the 1 ms hydrogen ionization period; however, it was not possible to store hydrogen ions and larger product ions together during the reaction period due to the large difference in m/z. Instead, the self-protonation product ion at m/z 3 was monitored during a reaction period varied between 0 and 40 ms over 14 scans each followed by an analytical scan from 2 to 5 Th in 0.18 ms.
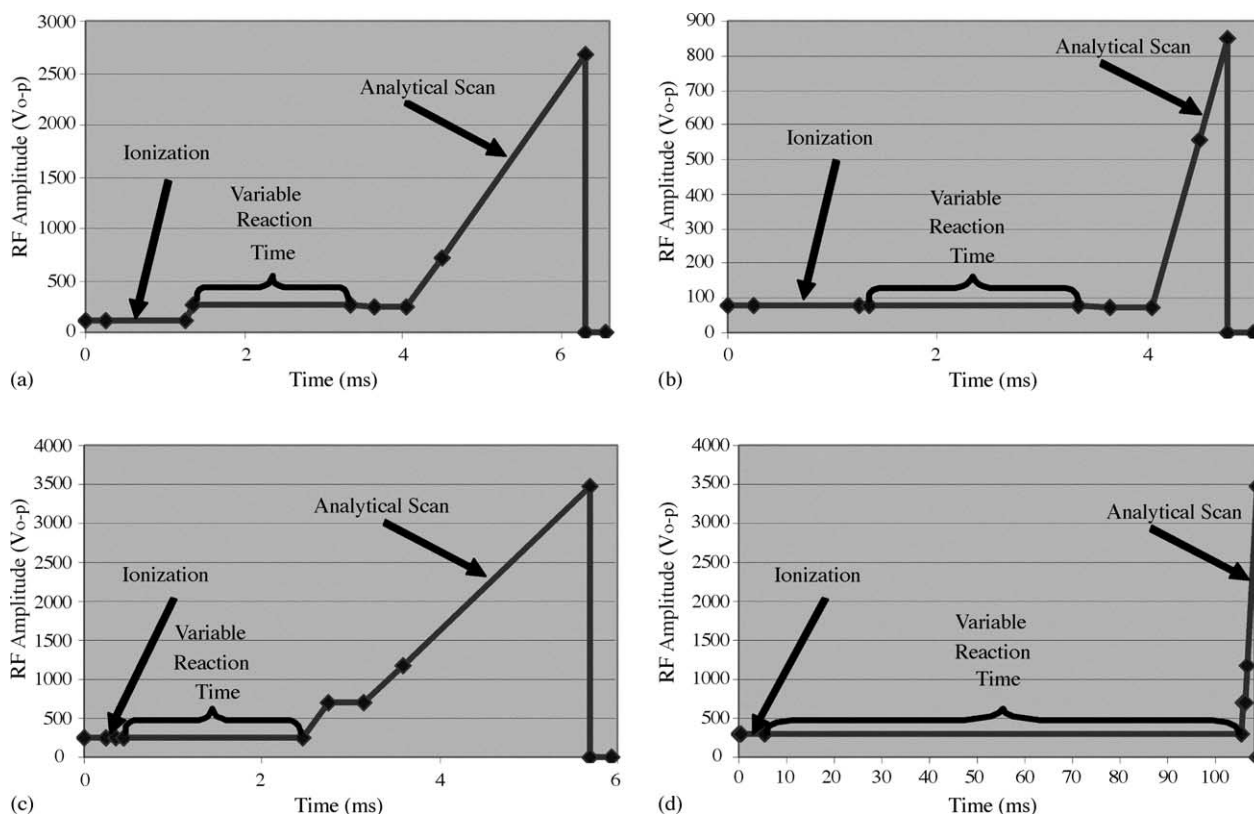

Fig. 2. Customized QITMS scan functions used in reaction experiments: (a) helium ions were collected during a 1 ms ionization period, and then reacted with background gas (predominantly nitrogen) over a variable reaction period. Product ions between 4 and 32 Th were mass analyzed; (b) hydrogen ions collected over a 1 ms ionization period were reacted with hydrogen neutrals, forming protonation products, which were mass analyzed between 2 and 5 Th; (c) argon ions collected over a 0.1 ms ionization period were reacted with ambient water during a variable reaction period, and product ions between 10 and 45 Th were mass analyzed. The scan function was also used for nitrogen ions to estimate the ambient water concentration inside the vacuum chamber. In (a)–(c) the variable reaction time is shown as a 1 ms event. The actual duration was varied in multiple scans as described in the text. (d) The ion-molecule reaction end products between background gases were determined by using long variable reaction times depicted here as a 100 ms period to emphasize the long duration. This allowed thermodynamic equilibrium to be established.

Table 2
Repetitive ion-molecule reaction experiments between He$^{\bullet+}$ and N$_2$

Criteria	Run 1	Run 2	Run 3	(1/2) × He pressure	2 × He pressure	(2/3) × N$_2$ pressure	(4/3) × N$_2$ pressure
Chamber temperature (K)	297	297	297	302	302	302	302
BG pressure (Torr)	5.8×10^{-7}	5.8×10^{-7}	5.7×10^{-7}	5.7×10^{-7}	5.7×10^{-7}	5.7×10^{-7}	5.7×10^{-7}
He pressure, main inlet (Torr)	2.7×10^{-7}	2.6×10^{-7}	2.5×10^{-7}	1.3×10^{-7}	5.3×10^{-7}	2.6×10^{-7}	2.6×10^{-7}
N$_2$ pressure, auxiliary port (Torr)	7.4×10^{-6}	7.4×10^{-6}	7.4×10^{-6}	7.4×10^{-6}	7.4×10^{-6}	4.9×10^{-6}	9.9×10^{-6}
N_d of added N$_2$ (molecule/cm^3)	2.4×10^{11}	2.4×10^{11}	2.4×10^{11}	2.4×10^{11}	2.4×10^{11}	1.6×10^{11}	3.2×10^{11}
N_d of BG (molecule/cm^3)	1.9×10^{10}	1.9×10^{10}	1.8×10^{10}	1.8×10^{10}	1.8×10^{10}	1.8×10^{10}	1.8×10^{10}
Reaction rate, $-\ln \Delta$He$^{\bullet+}$ (s^{-1})	421	412	410	409	437	296	574
k (using N$_2$ only, cm^3/s molecule)	1.8×10^{-9}	1.8×10^{-9}	1.7×10^{-9}	1.7×10^{-9}	1.8×10^{-9}	1.9×10^{-9}	1.8×10^{-9}
k (N$_2$ + 50% BG, cm^3/s molecule)	1.7×10^{-9}	1.7×10^{-9}	1.7×10^{-9}	1.7×10^{-9}	1.8×10^{-9}	1.8×10^{-9}	1.8×10^{-9}

Argon ions with ambient water was performed using the scan function in Fig. 2c. The argon pressure was increased to provide a background pressure of 7×10^{-6} Torr in the absence of the normal nitrogen background. A short ionization period of 0.1 ms was required to minimize space charge with the high analyte pressure. Argon ions were held at a low q_z of 0.091 to effectively trap lower mass product ions during the reaction period varied from 0 and 60 ms in 10 scans. Ions between 10 and 45 Th were mass analyzed within 2.10 ms.

The scan function in Fig. 2d was used in determining thermodynamic end products of ionized background gas (BG). A long ionization period of 5 ms was required for adequate ion production at lower pressure. Reaction periods varied from 0 to 4000 ms over nine scans ensured thermodynamic equilibrium. Ions between 10 and 45 Th were mass analyzed within 2.10 ms.

3. Results and discussion

3.1. He$^{\bullet+}$ reactions

The complex dynamics between reactant helium ions and background neutrals are illustrated in Fig. 3a. The helium ion signal intensity decreased rapidly as signals for nitrogen ions increased. The reaction was exothermic, $\Delta H = -9$ eV, with enough energy to break apart the nitrogen diatomic bond (9 eV [17]), explaining production of atomic and molecular ions. Nitrogen ions underwent subsequent charge-exchange reactions with water to produce the ion signal at m/z 18. The hydronium ion signal intensity at m/z 19 also increased as more water ions became available for self-protonation. Charge-exchange between helium ions and water neutrals was not observed, since the reaction was highly exothermic at -12 eV, leading to fragmentation of the 5 eV hydrogen–oxygen bonds. The oxygen ion signal intensity at m/z 32 increased as most ions charge-exchange with oxygen. Protonated nitrogen at m/z 29 also increased through reaction with background hydrogen.
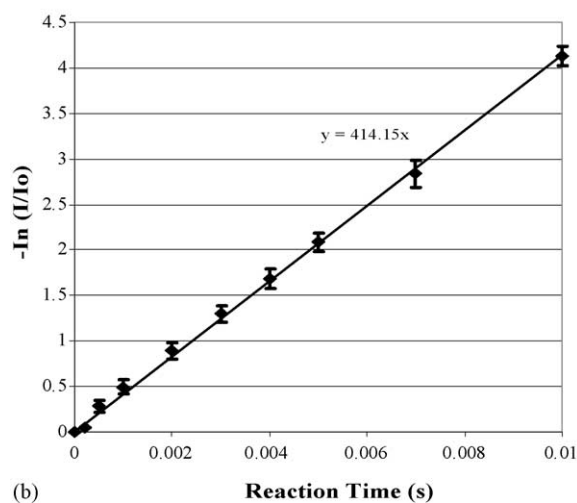
Data from the reaction of helium ions with nitrogen gas was acquired in triplicate as summarized in Table 2. Using Eq. (1) and the change in $\ln(I/I_0)$ versus time from Fig. 3b, the rate constant was calculated to be

1.7×10^{-9} cm^3/s molecule, matching the Langevin estimation of $k_L = 1.7 \times 10^{-9}$ cm^3/s molecule, which was close to the literature value of $k = 1.75 \times 10^{-9}$ cm^3/s molecule [29].

We report a second rate constant accounting for nitrogen gas present in the chamber background. Atmospheric air
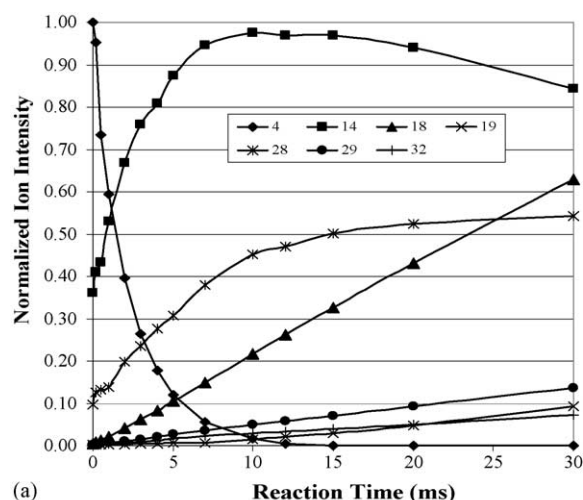
Fig. 3. Reaction data of helium ions with background gases: (a) ion intensities vs. reaction time for the reaction of He$^{\bullet+}$ and background gases; (b) plot of change in helium ion signal intensity vs. reaction time. Data points are the average of three repetitive runs, with error bars of 1σ.

leaking into the chamber from the inlet block (rough pumped to 20 mTorr) increased the chamber pressure from 2×10^{-8} to 6×10^{-7} Torr when the inlet was opened. Through analysis of background mass spectra, we assumed 50% of the increased pressure was from nitrogen. The new rate constant was slightly lower as shown in Table 2, since significantly less nitrogen was present in the background than was intentionally added for the experiment.

Next, the effect of changing helium or nitrogen pressure was studied (see Table 2). The helium pressure when changed to half or twice the initial pressure had only a minor (<5%) effect on reaction rate explained by changes in the ion collisional cooling rate. In contrast, nitrogen pressure significantly impacted the reaction rate: at 1.33 times the nitrogen pressure the rate increased by 39%. The reaction between helium ions and nitrogen was confirmed to be pseudo-first order as evident by the rate constant remaining unchanged at $1.8 \pm 0.1 \times 10^{-9}$ cm^3/s molecule.

Inlets for the helium and nitrogen gas plumbing were reversed to verify the ion trap pressure calculation. The reaction rate changed only 3%, without any change in the rate constant indicating that the experimental results were unaffected by the plumbing configuration. Having validated our main inlet pressure correction factors, they were applied for all later experiments.

In summary, the results demonstrated that helium ions react with nitrogen at the collision rate. The half-life of helium ions inside the ion trap was 1.8 ms at room temperature and a nitrogen pressure of 7×10^{-6} Torr. Under these conditions, 98% of trapped helium ions would be neutralized during a scan cycle of 10 ms, dramatically reducing sensitivity.

3.2. $H_2^{\bullet+}$ self-protonation and other reactions

Reaction between hydrogen ions and nitrogen was difficult to study, given that both proton transfer and charge-exchange occurred, being exothermic by -0.55 eV and between -0.8 and -1.8 eV, respectively. Additionally, reaction products could not be trapped while storing hydrogen ions due to the large mass difference. However, the competing reaction of hydrogen self-protonation forming H_3^+ was studied while admitting only hydrogen gas (Fig. 4a). The rate constant of this rapid reaction was determined to be 3.3×10^{-9} cm^3/s molecule, not matching either the Langevin approximation $k_L = 2.1 \times 10^{-9}$ cm^3/s molecule or literature values ranging from 2.08 to 2.12×10^{-9} cm^3/s molecule [29]. The experimental rate constant was elevated due to the neutralization of hydrogen ions through reactions with background species that were also rapid in nature: nitrogen, $k = 2.8 \times 10^{-9}$ cm^3/s molecule; water, $k = 5.37 \times 10^{-9}$ cm^3/s molecule; and oxygen, $k = 7.56 \times 10^{-9}$ cm^3/s molecule. These reactions increased the rate of hydrogen ion loss, skewing the calculated self-protonation rate constant. The multitude of alternative reaction pathways were difficult to distinguish from one another. They can be characterized
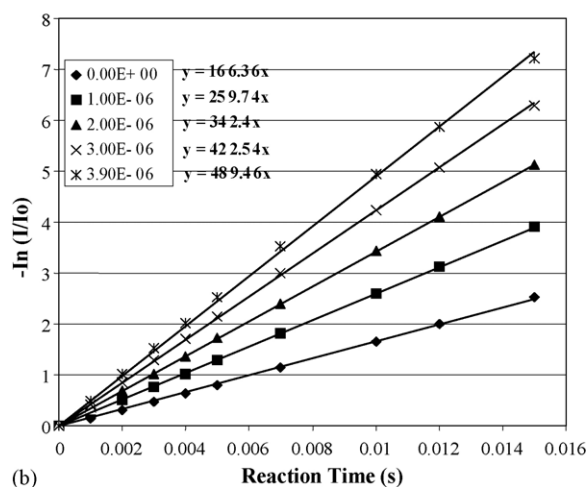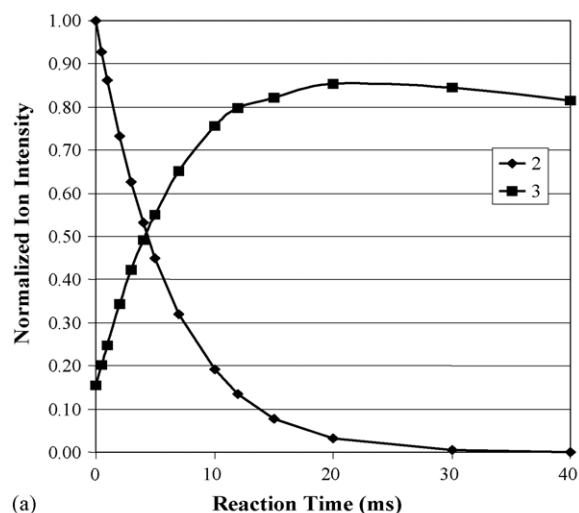

(a)

(b)

Fig. 4. Hydrogen ion reaction data: (a) ion intensity vs. reaction time for the self-protonation reaction of H_2 to form the $H_3^{\bullet+}$ ion at m/z 3; (b) five plots of change in hydrogen ion signal intensity vs. reaction time each at a different partial pressure of nitrogen inside the ion trap.

together as

$$(N_D k)_{\text{Total}} = \sum_1^n (N_D k)_n \tag{5}$$

which is useful when the number densities of each gas is accurately known. Since this was not the case, the self-protonation rate constant was determined with Eq. (6):

$$k = -\ln\left(1 - \frac{[H_3^+]_t}{[H_3^{\bullet+}]_0}\right) \frac{1}{[H_2]t} \tag{6}$$

a valid approximation since the product ion was exclusively produced by self-protonation. The H_3^+ appearance rate was slower than the hydrogen ion loss, as no competing reactions were involved. The determined rate constant of 2.2×10^{-9} cm^3/s molecule closely matched the approximated value and the average of the literature values at 2.1×10^{-9} [29].

Table 3
Hydrogen ion-molecule reaction at different N_2 pressures

Criteria	No N_2 added	First N_2 pressure	Second N_2 pressure	Third N_2 pressure	Fourth N_2 pressure
Chamber temperature (K)	297	297	297	297	297
BG pressure (Torr)	3.8×10^{-7}	3.5×10^{-7}	3.5×10^{-7}	3.5×10^{-7}	3.5×10^{-7}
H_2 pressure, main inlet (Torr)	1.6×10^{-6}	1.6×10^{-6}	1.6×10^{-6}	1.6×10^{-6}	1.6×10^{-6}
N_2 pressure, auxiliary port (Torr)	0	1.0×10^{-6}	2.0×10^{-6}	3.0×10^{-6}	3.9×10^{-6}
Reaction rate, $-\ln \Delta H_2^{\bullet+}$ (s^{-1})	166	260	342	423	489
k ($H_2^{\bullet+} + N_2$, cm^3/s molecule)	–	2.8×10^{-9}	2.7×10^{-9}	2.6×10^{-9}	2.6×10^{-9}

Though self-protonation affects hydrogen analysis at a high hydrogen concentration, this was of lesser concern than reaction with nitrogen, predominant in the purged Space Shuttle compartments, since NASA would abort a launch when observing even a modest rise in hydrogen. To evaluate these reactions, hydrogen ion loss was monitored at five different nitrogen pressures as detailed in Table 3. Rate constants were determined at each pressure using Eq. (5) and the reaction rate plots in Fig. 4b. The average, 2.7×10^{-9} cm^3/s molecule, was close to a value from the literature $(2.8 \pm 0.2) \times 10^{-9}$ cm^3/s molecule [29], but higher than the approximation $k_L = 2.3 \times 10^{-9}$ cm^3/s molecule. Under normal operation with a nitrogen background of 7×10^{-6} Torr the half-life of hydrogen ions was 1.1 ms, where 99.8% of trapped hydrogen ions would be lost during a scan cycle of 10 ms.

3.3. Reactions with H_2O

Water, with the highest proton affinity of the studied gases was a significant contaminant, reacting with other gases by proton transfer and hydrogen-atom transfer. With a low ionization energy, water also readily charge-exchanged with all ions except oxygen. Considering this reactivity, it is expected that a high water concentration would adversely affect analytical performance.

Thirty-five percent of the ion trap background pressure was attributed to water as observed in background mass spectra. Additional verification was observed by monitoring the reaction of nitrogen ions with background water. The reaction rate was slow (Table 4) because of the low water concentration. With a rate constant of 2.3×10^{-9} cm^3/s molecule, the average of reported literature values [29], the calculated water partial pressure was 1.3×10^{-7} Torr, or 32.5% of the BG pressure, agreeing with the earlier prediction, and was used to study argon ion reactions below.
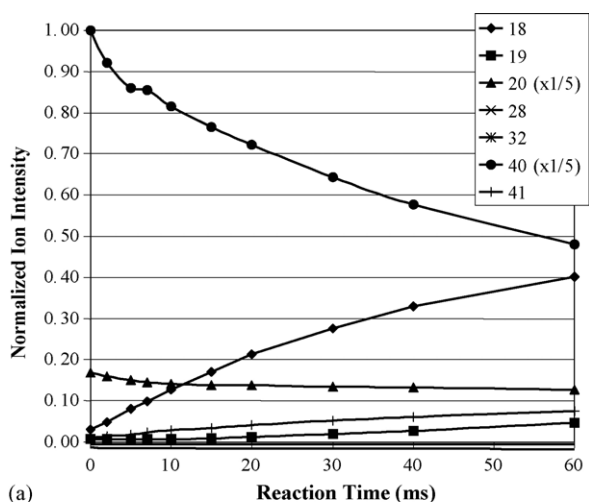
3.4. $Ar^{\bullet+}$ reactions

The ion-molecule reaction of argon ions with nitrogen was marginally exothermic ($\Delta H = -0.2$ eV). The reaction had already been studied by QITMS and other techniques [29], and was known to be slow, with a rate constant between 1.0×10^{-11} and 7.0×10^{-12} cm^3/s molecule. In contrast, argon ions readily charge-exchanged with water as illustrated in Fig. 5a. Products from charge-exchange and hydrogen-atom transfer were observed at m/z 18 and 41, respectively. The ion signal intensity for the doubly charged form of argon

Table 4
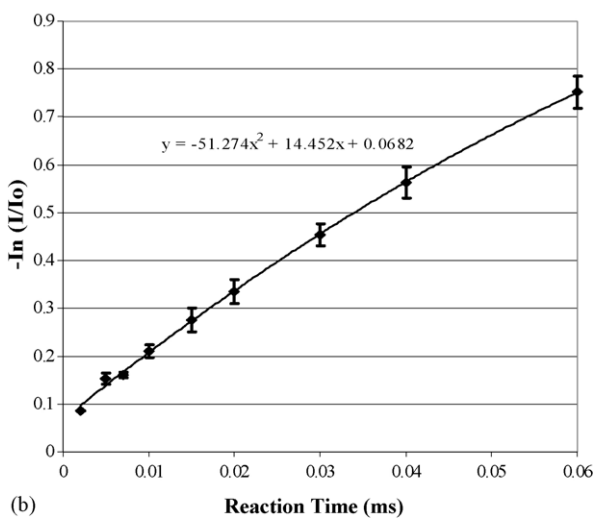Determination of water vapor pressure via reaction with $N_2^{\bullet+}$; three replicate runs

Criteria	Run 1	Run 2	Run 3
Chamber temperature (K)	297	297	297
BG pressure (Torr)	4.0×10^{-7}	4.0×10^{-7}	4.0×10^{-7}
N_2 pressure, auxiliary port (Torr)	7.2×10^{-6}	7.1×10^{-6}	7.0×10^{-6}
N_d of BG (molecule/cm^3)	1.3×10^{10}	1.3×10^{10}	1.3×10^{10}
Reaction rate, $-\ln \Delta H_2^{\bullet+}$ (s^{-1})	10.1	9.75	9.70
N_d of H_2O (molecule/cm^3)	4.4×10^9	4.2×10^9	4.2×10^9
H_2O pressure (Torr)	1.4×10^{-7}	1.3×10^{-7}	1.3×10^{-7}

Table 5
Ion-molecule reaction between argon ions and water; three replicate runs

Criteria	Run 1	Run 2	Run 3
Chamber temperature (K)	297	297	297
BG pressure (Torr)	4.0×10^{-7}	4.0×10^{-7}	4.0×10^{-7}
Ar pressure, main inlet (Torr)	7.2×10^{-6}	7.2×10^{-6}	7.2×10^{-6}
N_d of added Ar (molecule/cm^3)	2.3×10^{11}	2.3×10^{11}	2.3×10^{11}
N_d of H_2O (molecule/cm^3)	4.3×10^9	4.3×10^9	4.3×10^9
Reaction rate, $-\ln \Delta H_2^{\bullet+}$ (s^{-1})	13.6	14	14.2
k using H_2O (cm^3/s molecule)	3.2×10^{-9}	3.3×10^{-9}	3.3×10^{-9}

(a)

(b)

Fig. 5. Argon ion reaction data: (a) ion intensities vs. reaction time for the reaction of $Ar^{\bullet+}$ with background gas; (b) plot of change in argon ion signal intensity (singly charged) vs. reaction time. Data points are the average of three repetitive runs, with error bars of 1σ. Trend is shown to be quadratic in nature.

Fig. 6. Monitored ion signals of background gases (4.0×10^{-7} Torr) as the reaction time was incremented from 0 to 4000 ms. Thermodynamic equilibrium was reached after 2000 ms, with only signals for hydronium and oxygen ions remaining.

by the quadratic trend in argon ion loss shown in Fig. 5b. This indicates a second reaction pathway, likely that which forms ArH^+, observed at m/z 41 in Fig. 5a. Ruling out proton transfer due to the low proton affinity of Ar (Table 1), hydrogen-atom transfers from either background water or hydrogen are possibilities. At this point the formation of the signal at m/z 41 remains unclear.

The partial pressure of water was kept low in our experiments. At a water pressure of 1.3×10^{-7} Torr, argon ions had a half-life of 33 ms, three times the scan cycle. The concentration of water sampled from the Space Shuttle, in contrast would be sporadic while on the launch pad; thereby, this reaction would affect sensitivity and signal stability for argon monitoring.

3.5. Thermodynamics of $O_2^{\bullet+}$ and H_3O^+

The oxygen ion signal was the only one of four analytes monitored in this study that was not reduced through reactions with background gases. In fact, the oxygen ion signal intensity increases as shown in Fig. 6 at thermodynamic equilibrium (>2 s reaction time). Oxygen has a low ionization energy; therefore, other ions (to include hydrogen, helium, and argon analyte ions) will charge-exchange with background oxygen, increasing the oxygen ion signal intensity as other ions are depleted. This partially explains the reduction of ion signal intensity for atomic and diatomic nitrogen ions at m/z 14 and 28, respectively, and for argon ions at m/z 40.

The hydronium ion at m/z 19 was the only other ion remaining at thermodynamic equilibrium. It has a lower

(Ar^{2+}) at m/z 20 is also shown to diminish in Fig. 5a through charge-exchange with water. This is of less significance as only a small amount of doubly charged argon is formed by electron impact ionization. The absence of signal at 28 and 32 Th indicated that reactions with nitrogen and oxygen were much slower with comparable concentrations.

Using the previously determined water pressure of 1.3×10^{-7} Torr (background ion trap pressure remained constant) a rate constant of 3.3×10^{-9} cm³/s molecule was calculated (Table 5 and Fig. 5b). The value was higher than both the ADO approximation for polar neutrals of $k_{ADO} = 2.0 \times 10^{-9}$ cm³/s molecule and literature values ranging from 1.0×10^{-9} and 2.1×10^{-9} cm³/s molecule [29]. Another reaction that partially explains the higher rate constant would be charge-exchange with background hydrogen. The complicated nature of this reaction system is illustrated
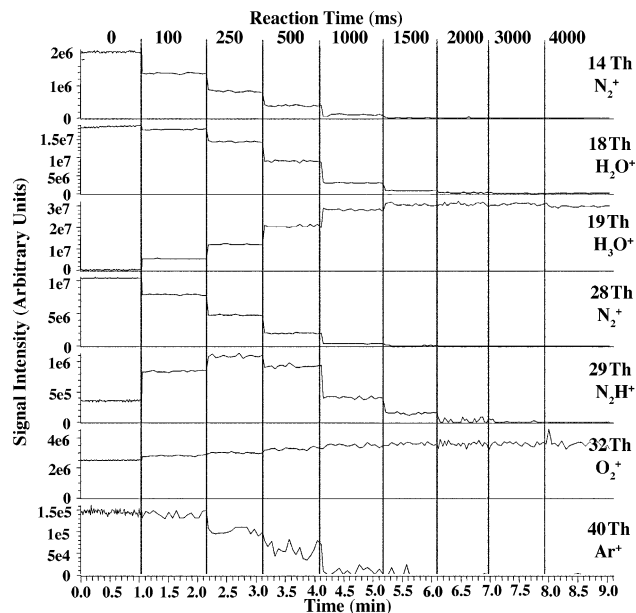
recombination energy than oxygen's ionization energy. Water, also with a low ionization energy, is readily ionized through charge-exchange with other ions. Hydronium ions are primarily generated through the self-protonation of water, though a lesser amount is formed by reactions with other Brønsted acid ions such as $H_2^{\bullet+}$ and N_2H^+ each with lower proton affinities than water.

As evident in Fig. 6, a long reaction period was required to reach thermodynamic equilibrium under normal experimental conditions. These same thermodynamically favored ions were prevalent for hours following vacuum chamber evacuation even with very short ionization periods. Water is pumped away slowly as the chamber is placed under vacuum (a few hours with our small vacuum chamber and open ion trap configuration). To meet NASA requirements, this process was sped up by baking the chamber during evacuation. Baking will not, however, control water being sampled from inside the Space Shuttle, a potential problem in this application.

4. Conclusions

Ion-molecule reactions had a significant effect on the analytical performance of QITMS when analyzing permanent gases. Hydrogen and helium ions reacted rapidly in the predominantly nitrogen background, reducing ion intensity by 50% within 1–2 ms and considerably affecting sensitivity during the 10–20 ms scan time. Argon and hydrogen ions reacted readily with background water through proton transfer, which makes the QITMS sensitive to environmental changes. Oxygen ions were thermodynamically favored through exothermic charge-exchange reactions with the three other analytes and background nitrogen. Thus a sharp rise in another analyte would also present an increased oxygen ion signal intensity.

Negative effects of ion-molecule reactions were eventually mitigated by controlling time and pressure inside the ion trap. With proper adjustment of scan function timing and gas conductance into the ion trap, the QITMS was able to operate at nitrogen and water pressures typical for the inner compartments of the Space Shuttle, with a minimal sacrifice in analytical performance. The technology was successfully applied to the AHGD project application, meeting NASA's requirements [5] for monitoring hydrogen, helium, oxygen and argon levels.

References

[1] G.R. Naylor, R. Hritz, T. Greenfield, C. Lampkin, F. Lorenzo-Luaces, L. Lingvay, D. Floyd, F. Adams, G. Breznik, B. Davis, A. Schwalb, C. Curley, G. McKinney, NASA Technical Briefs, May 2001.

[2] W.R. Helms, S.O. Starr, The 33rd Space Congress on Advanced Development of Ground Instrumentation as a Key Strategy in Improving the Safety and Efficiency of Space Shuttle Checkout and Launch, Cocoa Beach, FL, 1996.

[3] T.P. Griffin, G.S. Breznik, C.A. Mizell, W.R. Helms, G.R. Naylor, W.D. Haskell, Trends Anal. Chem. 21 (2002) 488.

[4] A.K. Ottens, W.W. Harrison, T.P. Griffin, W.R. Helms, J. Am. Soc. Mass Spectrom. 13 (2002) 1120.

[5] C.R. Arkin, T.P. Griffin, A.K. Ottens, J.A. Diaz, D.W. Follistein, F.W. Adams, W.R. Helms, J. Am. Soc. Mass Spectrom. 13 (2002) 1004.

[6] A.G. Harrison, Chemical Ionization Mass Spectrometry, CRC Press, Boca Raton, FL, 1992.

[7] P. Liere, V. Steiner, K.R. Jennings, R.E. March, J.C. Tabet, Int. J. Mass Spectrom. Ion Process. 167–168 (1997) 735.

[8] G.L. Glish, S.A. McLuckey, Int. J. Mass Spectrom. Ion Process. 106 (1991) vii.

[9] B.D. Nourse, R.G. Cooks, Anal. Chim. Acta 228 (1990) 1.

[10] G. Lawson, J.F.J. Todd, British Mass Spectroscopy Group Meeting, Bristol, 1971 (abstract No. 44).

[11] R.F. Bonner, G. Lawson, J.F.J. Todd, Int. J. Mass Spectrom. Ion Phys. 10 (1972–1973) 197.

[12] B.A. Eckenrode, S.A. McLuckey, G.L. Glish, Int. J. Mass Spectrom. Ion Process. 106 (1991) 137.

[13] R.E. March, R.J. Hughes, J.F.J. Todd, Quadrupole Storage Mass Spectrometry, Wiley/Interscience, New York, NY, 1989.

[14] A.B. Weglein, D. Rapp, in: M.T. Bowers (Ed.), Gas Phase Ion Chemistry, vol. 2, Academic Press, New York, NY, 1979, p. 300 (Chapter 16).

[15] E. Lindholm, in: P.J. Ausloos (Ed.), Ion-Molecule Reactions in the Gas Phase, American Chemical Society, Washington, DC, 1966, p. 1 (Chapter 1).

[16] E. Lindholm, in: J.L. Franklin (Ed.), Ion-Molecule Reactions, vol. 2, Plenum Press, New York, NY, 1972, p. 457 (Chapter 10).

[17] D.R. Lide (Ed.), CRC Handbook of Chemistry and Physics, 71st ed., CRC press, Boca Raton, FL, 1990.

[18] E.P.L. Hunter, S.G. Lias, J. Phys. Chem. Ref. Data 27 (1998) 413.

[19] J.L. Franklin, M.A. Haney, in: J.L. Franklin (Ed.), Ion-Molecule Reactions. Part II. Evaluated Pressures and Long Reaction Times, Dowden, Hutchinson and Ross, Stroudsburg, PA, 1979, p. 233 (Chapter 26).

[20] J.A. de Gouw, L.N. Ding, M.J. Frost, S. Kato, V.M. Bierbaum, S.R. Leone, Chem. Phys. Lett. 240 (1995) 362.

[21] W.J. Knott, D. Proch, K.L. Kompa, C. Rose-Petruck, J. Chem. Phys. 102 (1995) 214.

[22] E.M. Snyder, A.W. Castleman Jr., J. Chem. Phys. 107 (1997) 744.

[23] W.J. Knott, D. Proch, K.L. Kompa, J. Chem. Phys. 108 (1998) 527.

[24] E.J. Hunter, A.R. Homyak, S.N. Ketkar, J. Vac. Sci. Technol. A 16 (1998) 3127.

[25] S.A. McLuckey, G.L. Glish, K.G. Asano, G.J. Van Berkel, Anal. Chem. 60 (1988) 2312.

[26] S.N. Ketkar, A.D. Scott Jr., E.J. Hunter, Int. J. Mass Spectrom. 206 (2001) 7.

[27] T. Su, M.T. Bowers, in: M.T. Bowers (Ed.), Gas Phase Ion Chemistry, vol. 1, Academic Press, New York, NY, 1979, p. 83 (Chapter 3).

[28] W. Lindinger, in: J.H. Futrell (Ed.), Gaseous Ion Chemistry and Mass Spectrometry, Wiley/Interscience, New York, NY, 1986, p. 237 (Chapter 11).

[29] Y. Ikezoe, S. Matsuoka, M. Takebe, A. Viggiano, Gas Phase Ion-Molecule Reaction Rate Constants through 1986, Maruzen Company, Tokyo, Japan, 1987.